

A Simulation Study of Cooperative Communications over HF Channels

by

Mohammed Jameel Hakeem

A thesis
presented to the University of Waterloo
in fulfillment of the
thesis requirement for the degree of
Master of Applied Science
in
Electrical and Computer Engineering
Waterloo, Ontario, Canada, 2008

© Mohammed Jameel Hakeem 2008

AUTHOR'S DECLARATION

I hereby declare that I am the sole author of this thesis. This is a true copy of the thesis, including any required final revisions, as accepted by my examiners.

I understand that my thesis may be made electronically available to the public.

Abstract

The High Frequency (HF) band lies within 2-30 MHz of the electromagnetic spectrum. In this part of the spectrum, propagation via direct wave, surface wave, and ionospheric refraction mechanisms provides means of communications from line-of-sight to beyond-line-of-sight ranges. The characteristics of ionospheric channel impose fundamental limitations on the performance of HF communication systems. The major impairment is fading which results in random fluctuations in the received signal level and affects the instantaneous signal-to-noise ratio. This requires the deployment of powerful diversity techniques to mitigate the degrading effects of fading on the performance. The range of wavelengths in HF band unfortunately restricts the use of spatial diversity (i.e., deployment of multiple antennas) for most practical purposes. This thesis focuses on an alternative method to exploit the spatial dimension of the HF channel. Specifically, we aim to extract distributed spatial diversity through relay-assisted transmission. Towards this main goal, we consider multi-carrier HF communication and investigate the performance of cooperative OFDM over HF channels.

Acknowledgements

Although I am indeed the sole author of this thesis, as customarily declared in the beginning, I am surely not the sole contributor. So many people have contributed to my thesis, to my education, and to my life, and it is now my great pleasure to take this opportunity to thank them.

I would like to start my acknowledgment to thank the government of the Kingdom of Saudi Arabia; particularly the Ministry of Higher Education along with the Saudi Arabian Cultural Bureau in Ottawa for giving me the opportunity to make my dream come true of seeking a graduate degree.

I would like to express my deepest and sincere gratitude to my supervisor, Professor Murat Uysal. His valuable support, guidance, and encouragement have been vital to me in pursuing my degree. Professor Uysal is truly an endless source of creative ideas. His great effort and advice helped me learn valuable lessons which would definitely help me in my future career. He is an ideal role model for aspiring scientists and academicians.

I would also like to thank my colleagues Dr. Yanwu Ding, Dr. Hakam Mheidat, Mehboob Fareed, Osama Amin, Majid Safari, Suhail Al-Dharrab, and Jawad Hussain who provided an endless source of support and inspiration. I also would like to extend my special sincere thanks to my roommate Saad Alaboodi and to all my friends for all their great advice and support.

Finally, my deepest thanks go to my dad Jameel Hakeem and my mom Najya Alrodainy, who taught me great lessons and were the greatest support in my life, without them and their prayers I won't be where I am right now. They are God's gift to me in my life.

Dedication

To my parents: Jameel and Najya

Table of Contents

AUTHOR'S DECLARATION	ii
Abstract	iii
Acknowledgements	iv
Dedication	v
Table of Contents	vi
List of Figures	vii
List of Tables	viii
Chapter 1 Introduction to HF Communications.....	1
1.1 History of HF Communications	1
1.2 The Structure of Ionosphere	3
1.3 Propagation in HF Band.....	6
1.3.1 Sky Wave Propagation	6
1.3.2 Ground Wave Propagation	7
1.3.3 HF Propagation Ranges	9
1.4 Application Areas of HF Communications.....	10
Chapter 2 Fading Mitigation in HF Channel	13
2.1 Fading Channel Model for HF Propagation.....	13
2.2 Diversity Techniques.....	16
2.2.1 Frequency Diversity	17
2.2.2 Time Diversity	17
2.2.3 Space (Antenna) Diversity.....	17
2.2.4 Polarization Diversity	18
2.3 Cooperative Diversity	18
2.4 Motivation and Thesis Objective	20
Chapter 3 Cooperative OFDM for HF Communications.....	23
3.1 Transmission Model.....	24
3.2 Simulation Results and Discussion	30
Chapter 4 Conclusions	38
Bibliography	40

List of Figures

Figure 1.1: Determination of the ionosphere by measuring the angle of arrival.....	2
Figure 1.2: Ionospheric layers [4].	5
Figure 1.3: Sky wave propagation.....	7
Figure 1.4: Ground wave propagation.....	8
Figure 1.5: HF propagation distinct ranges	10
Figure 2.1: HF Radio Wave Propagation Modes	13
Figure 2.2: Watterson HF Tapped Line Model	14
Figure 2.3: Tap Gain Spectrum for different HF modes	15
Figure 3.1 Single-relay network.	24
Figure 3.2 Frame structure for OFDM with pilot symbols inserted in time and frequency domains.....	26
Figure 3.3 Performance of SISO OFDM over HF channels with perfect channel estimation. .	31
Figure 3.4 Performance of SISO OFDM over HF channels with imperfect channel estimation.	32
Figure 3.5: Effect of channel estimation on the performance of SISO OFDM for different Doppler shifts (Good HF channel)	32
Figure 3.6 Effect of channel estimation on the performance of SISO OFDM for different Doppler shifts (Good HF channel).	33
Figure 3.7 Performance of cooperative OFDM over HF channels with perfect channel estimation.	35
Figure 3.8 Performance of cooperative OFDM over HF channels with imperfect channel estimation.	35
Figure 3.9 Effect of channel lengths on the performance of cooperative OFDM (Good HF channel)	36
Figure 3.10 Effect of channel estimation on the performance of cooperative OFDM for different Doppler shifts (Good HF channel).....	36
Figure 3.11 Effect of channel estimation on the performance of cooperative OFDM for different Doppler shifts (Good HF channel).....	37
Figure 3.12 Effect of relay location on the performance of cooperative OFDM	37

List of Tables

Table 2.1: Poor, moderate and good HF channels [9]	16
Table 2.2: Cooperation protocols for a single-relay network where source, relay and destination terminals are denoted by S, R and D.	20
Table 3.1: Parameter α for different values of L	27

Chapter 1

Introduction to HF Communications

For decades, HF (high frequency) band has been recognized as the primary means for long-range wireless communications. The HF band lies within 2-30 MHz of the electromagnetic spectrum. In this part of the spectrum, propagation via direct wave, surface wave, and ionospheric refraction mechanisms provides means of communications from line-of-sight (LOS) to beyond-line-of-sight (BLOS) ranges [1]. Direct wave propagation supports LOS communication whereas the surface wave mechanism provides BLOS communication typically in the range of 100-150km or more based on the terrain conditions. To reach even larger distances, HF radio takes advantage of the ionospheric refraction from upper parts of the atmosphere (known as sky wave or ionospheric propagation) and allows over-the-horizon communications with nearly worldwide coverage.

1.1 History of HF Communications

HF communication has been an essential part of worldwide information transmission since the advent of radio. The history of radio communication through ionospheric propagation dates back to the 19th century. In 1860, James Clark Maxwell predicted the existence of electromagnetic waves, but did not realize the significance that his theory would have on future research [2]. His theory was later confirmed in 1887 by Heinrich Hertz's experiment which showed that charged objects and electric sparks are produced when illuminated by ultraviolet light. These sparks travel at the speed of light and can be reflected, focused, and refracted, forming electromagnetic waves. At the same time that Hertz confirmed the existence of the electromagnetic radio waves, Balfour Stewart found evidence for the existence of the ionosphere [2]. Stewart proposed that the sequential variation in the earth's magnetic field is explained by the air currents in the upper atmosphere; these act as conductors, generating electric currents as they pass through the earth's magnetic field. The first practical demonstration of Hertz's experiment was done by Alexander Popov in the early 1890's [2]. In 1894, he succeeded in

transmitting radio signals over short distances. By the time Popov implemented his radio receiver, another Italian inventor, Guglielmo Marconi, gained attention for his early work on radio telegraphy. In 1896, with several successive experiments for the British post office, Marconi was able to significantly increase the transmission distance which eventually led to the first trans-Atlantic transmission [2]. This took place on December 31st, 1901 when Marconi succeeded in transmitting and receiving a signal from England to Newfoundland.

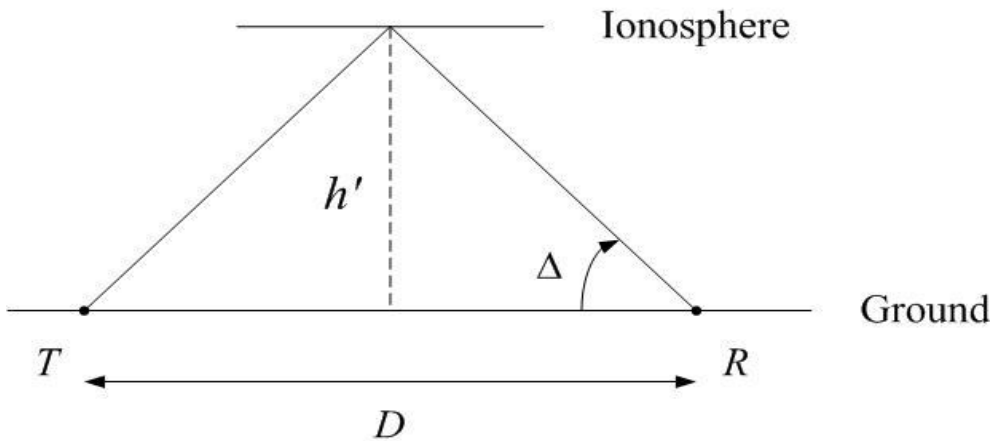


Figure 1.1: Determination of the ionosphere by measuring the angle of arrival.

After Marconi’s success, many others gained interest in this field. In 1902, Kennelly and Heaviside suggested that the cause behind Marconi’s transceiver success was the radio waves’ reflection back to the earth’s surface from an electrically conducting layer in the upper atmosphere. Kennelly and Heaviside’s remarkable observation on Marconi’s result led to the discovery of the HF radio propagation. Many experiments were carried out to determine the height of the Kennelly-Heaviside layer, as the ionosphere was then called. One of the main experiments was conducted by Edward Appleton in the 1920’s [2]. In his experiment, Appleton involved the measurement of the angle of arrival down-coming wave (see Figure 1.1). He

suggested that if the distance between the transmitter and the receiver is known, the height of the equivalent mirror reflector is given by [2]

$$h'_{\Delta} = \frac{1}{2} D \tan \Delta \quad (1.1)$$

where D represents the distance between the transmitter and the receiver and Δ is the arrival angle of the down-coming wave. By applying his experiment at different times, Appleton observed that the height of the reflector changed due to reflection from different layers located in the upper atmosphere; from this, the nature of the ionosphere along with the layers description were introduced.

Following Appleton's work, extensive studies and experiments were made on ionospheric radio propagation due to its increasing use in practice. By 1920's, propagation effects such as solar activities and magnetic storms were recognized and defined. In the beginning of 1930's, an ionosonde technique that is used to help in studying the ionosphere was developed. Different laboratories used this technique in analyzing the effect of the long-term variations in the ionosphere.

During World War II when many additional ionospheric base stations were built for mostly military communication, aspects of ionospheric study received much consideration. Through this network of base stations, the location control of the ionosphere was also detected. Many phenomena such as the irregular structure of the ionosphere, the fading of radio waves, and ionosphere absorption were also studied. In 1960's and 70's, the introduction of satellite and rockets led to further discoveries in ionospheric investigations by simplifying the measurements of air density, composition, electron density and the sun's ionizing radiation.

1.2 The Structure of Ionosphere

The ionosphere is the upper region of the earth's atmosphere, extending from roughly 50 km to 1000 km, in which sufficient numbers of ionization electrons exist to affect radio wave

propagation [2]. The source of ionization in the ionosphere is solar radiation also known as solar wind. When this radiation from the sun reaches the upper atmosphere region, it bombards gas molecules causing the electrons to expose from the atoms and consequently positively charged ion particles are produced. This process is known as ionization and the region of these electrically charged particles is known as the ionosphere.

The ionosphere is divided into three main layers: D, E and F (Figure 1.2). These layers are classified based on their electron density. The names of these layers were introduced by Appleton during his experiment and the descriptions are as follows:

The F layer: The F layer extends beyond 150 km to 400 km above the earth's surface. The central path of this layer has the greatest electron density in the earth's atmosphere, and ionization is essentially determined by dynamic processes. By the day-time hours, the layer is divided into two sub layers F1 and F2. On the other hand, during night hours, the F layer ionization is usually specified by as F2 layer [3].

The E layer (Electric field layer): The E layer is located in the center of the ionosphere from 90 km to 150 km in altitude. This layer has large amounts of electrons; however, their density is less compared to the F layer. This layer is practically weak at night, and the ionization of this layer is directly related to the zenith angle of the sun [3]. Sporadic E level occurs at the day time in some parts of the world and mainly at night in others, and it is produced by meteoric particles [2].

The D layer: The D layer is the lowest layer of the ionosphere and is located between 55 km and 90 km in altitude. It has weak ionization due to its position, and practically disappears at night [3]. This layer contains some free electrons and ions, but also many other molecules and atoms. The primary effect of this layer is to attract radiation; this occurs when the radiation interacts with an electron and causes the electron to move [3]. If the electron runs into a molecule, it is absorbed and so is the energy from radiation. The lower the frequency of transmission, the more the D layer absorbs the transmission energy [4].

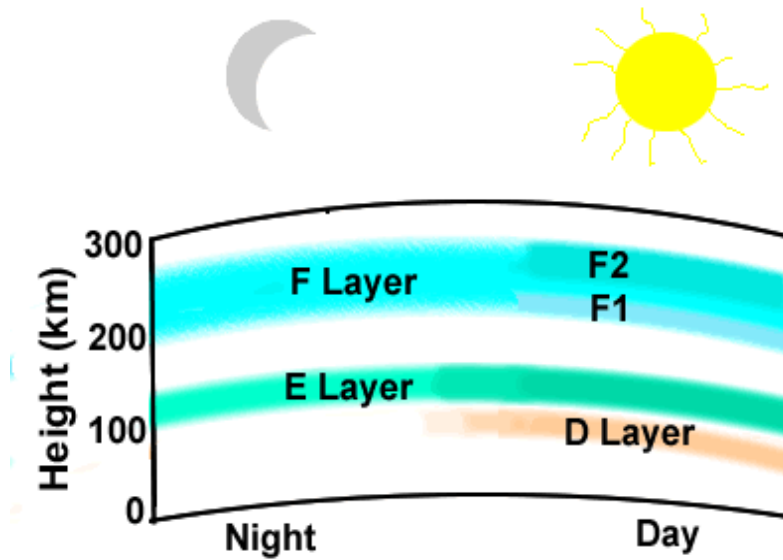


Figure 1.2: Ionospheric layers [4].

The existence of different layers in the ionosphere are due to the variations of the chemical composition of the air with height, and because the ability of different gases of the atmosphere to attract solar radiation at different frequencies varies within the ionosphere. Furthermore, the dielectric constant k , and the refraction index $n = \sqrt{k}$ of the air varies with height and, in general, decreases with increased height. The refractive index of the air is used to determine the behavior of the signal travelling in the atmosphere. So-called modified refractive index M is further defined as

$$M = \left(n - 1 + \frac{h}{a} \right) \times 10^6 \quad (1.2)$$

where n is the refraction index, h represents the height above the ground, and a is the radius of earth ($= 6.37 \times 10^6$ m). The variation dM/dh of M with height is an important factor in radio propagation. At high latitudes, the dielectric constant k and also n become independent of height. As a result, M increases 0.048 units per ft. At low latitudes and near the surface of the earth, the

dielectric constant decreases linearly with increasing height and hence, M increases linearly at a constant rate less than 0.048 units per ft. When the transmitted signal travels in the atmosphere, the change in the refractive index n with height causes the signal path to bend away from the regions of low dielectric constant toward regions of high dielectric constant. There are four possible cases that might occur, depending on the dielectric constant:

If the dielectric constant doesn't change with height, the radio wave will travel in a straight line and will be bent.

If the dielectric constant increases with height, in this case the wave path will bend away from the earth.

If the opposite, the dielectric constant decreases with height, the wave path will be bent, i.e., refracted towards the earth and allow long distance communications. This is a typical condition of the atmosphere.

If the dielectric constant decreases with height at a rate that keeps M constant $dM/dh = 0$, the curvature of the path will be similar to the earth's curve.

1.3 Propagation in HF Band

1.3.1 Sky Wave Propagation

Propagation in the HF channel mainly depends on the reflection of the radio waves from the ionosphere which is made up of one or more layers in the upper atmosphere. Those layers influence the radio waves mostly due to the movement of free electrons in the area. As described in Section 1.2 the ionosphere is divided into three layers or regions known as D, E and F respectively. Depending on certain conditions, sub-layers of these regions may exist; for example, sub-layers F1 and F2 in the F layer during day-light hours. The F and E layers act primarily as radio reflectors, whereas the D layer acts mainly as an absorber [1].

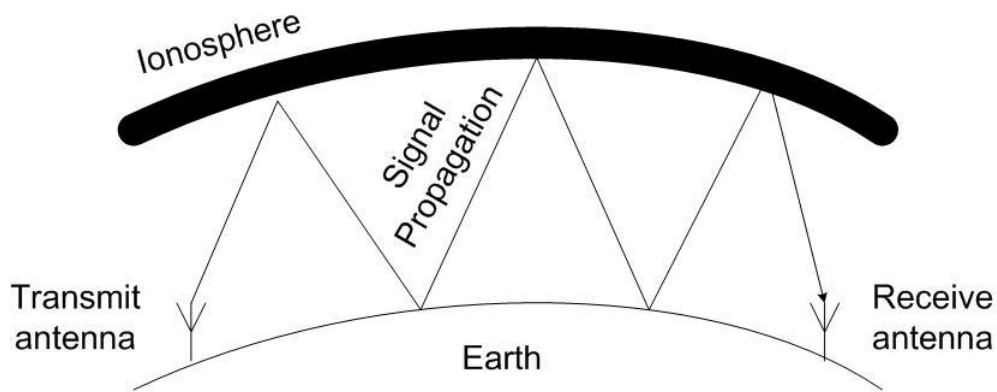


Figure 1.3: Sky wave propagation

Between the ionosphere and the Earth's surface signals travel back and forth in a number of hops and skips as shown in Figure 1.3. A reason for this is that the lower latitude layer (particularly the E-layer) largely disappears during night hours, causing the refractive layer of the ionosphere to be much higher. In sky wave propagation, the radio waves travel through the ionosphere's electric field and cause oscillatory motion in the electrons. This modifies the velocity of the propagation in the wave like miniature antennas by re-radiating. If the signal has low frequency, it will reflect back to the Earth's surface from the ionosphere due to the electron concentrations. If the Earth's magnetic field was absent, then the oscillatory motion of the electrons would be parallel to the direction of the electric field of the incident wave, and the re-radiate would have the same polarization as the incident wave [1]. On the other hand, when the Earth's magnetic field is present, it modifies the oscillatory motion of the electrons causing them to move in complex orbits. Their re-radiation in this case would not have the same polarization effect of the incident wave. Therefore the resultant wave polarization will change continuously as the wave crosses the ionosphere [1].

1.3.2 Ground Wave Propagation

For shorter distances and low frequencies (about less than 150 km), radio waves in HF transmission are directed via ground wave propagation (See Figure 1.4).

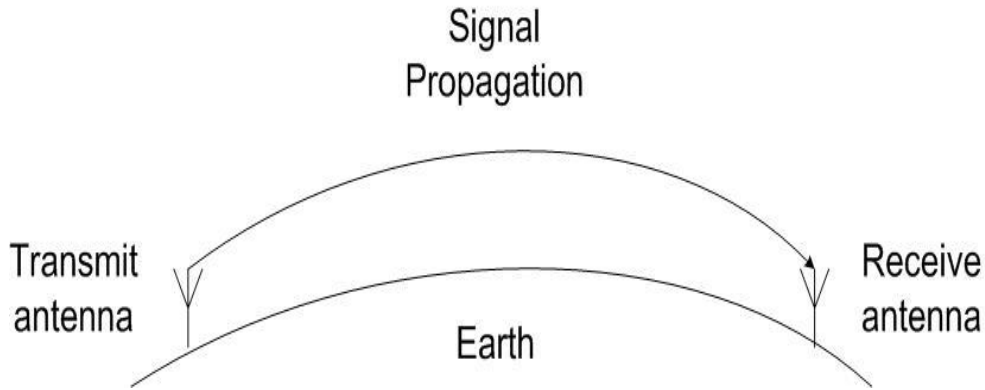


Figure 1.4: Ground wave propagation

The effects of electrical characteristics of ground propagation upon radio waves can be classified by the following equation

$$E/E_0 = \underbrace{1}_{\text{Direct Wave}} + \underbrace{R e^{i\Delta}}_{\text{Reflected Wave}} + \underbrace{1-R}_{\text{Surface Wave}} A e^{i\Delta} + \dots \quad (1.3)$$

where E/E_0 is defined as the ratio between the electrical field of the transmitted signal to the electrical intensity in the free space, R is the reflection coefficient of the ground for the wave polarization of interest, A is the surface wave attenuation factor, and Δ is the phase difference caused by the path difference between the direct and ground reflected waves [1]. From (1.3), two limiting cases can be considered which make the ground wave to either be purely surface wave or a space wave. In the first case, it is assumed that both the transceiver antennas are close to the ground level due to low grazing paths, Δ will approximately approach zero and the reflection coefficient becomes increasingly close to -1. As a result, the first two components in (1.3) will cancel, and the ground wave is then known as the surface wave. Moreover, the surface wave dominates because the Earth is not a perfect reflector, causing some energy to be transmitted into the ground. In the second case, if the transmitting and receiving antennas are above the ground

by a few wavelengths, the surface wave in (1.3) can be neglected, and the ground wave is called space wave (consisting of direct and reflected wave). (1.3) can be then written as

$$|E/E_0| = 2 \sin \Delta/2$$

(1.4)

1.3.3 HF Propagation Ranges

Based on the above discussions, the HF propagation can be identified by three distinct ranges depending on the importance of the ground and sky waves:

Ground waves occur in short ranges and using vertical polarization. With horizontal polarization no significant ground waves would take place.

For medium and long ranges and under the assumption of vertical polarization (and at ever range for horizontal polarization) the sky wave, if present, is the main model.

For intermediate ranges, there are two cases depending on the frequency of the signal and the existing ionosphere conditions:

Both ground and sky waves exist as shown in Figure 1.5 (a) with very strong fading if their mean values are equal.

A no wave or (silent zone) where the ground wave has been neglected and sky wave has not been shown yet as shown in Figure 1.5 (b).

It should be also noted that ground waves are just an attenuated, delayed version of the transmitted signal. However, sky waves, in addition of those two factors, are also subject to degrading effects such as frequency-selective and time-selective fading.

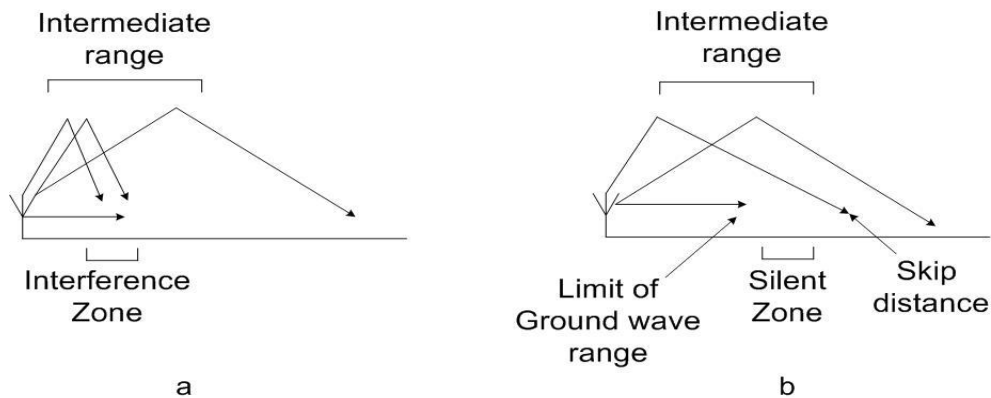


Figure 1.5: HF propagation distinct ranges

1.4 Application Areas of HF Communications

As a worldwide communication medium, spectrum utilization and allocation of HF band is regulated by the International Telecommunications Union (ITU) in Geneva. Allocations are made on the basis of service type which includes a wide range of applications some of which are elaborated in the following [1].

Aeronautical mobile systems: Radio communications between a land station and an aircraft, or between aircrafts

Maritime mobile: Radio communication between a cost station and ship, or between ships

Land mobile: Radio communication between a base station and a land mobile, or between land mobile stations

Broadcasting: Radio communication intended for direct reception by the general public. There exists a large number of broadcasting stations (e.g., Radio Canada International, BBC World Service, Voice of America) in HF band which are also known as “world band radio”. Until recently, analog modulation techniques have been employed for broadcasting in HF band. A new digital HF broadcasting standard known as Digital Radio Mondiale (DRM) was introduced in 2003.

Amateur (ham) radio: A portion of the HF band is allocated for the use of people interested in the radio technology as a hobby. An estimated six million people throughout the world are regularly involved with amateur radio.

Besides the above civilian purposes, HF communication is also widely used in military for both strategic and tactical communication. Strategic HF links are typically deployed between national command headquarters and forces located around the world. They are also used between airborne command posts, immediate warning and reconnaissance aircrafts, and national command posts [1]. Sky wave propagation, in general, is extensively used in data transmission in the military with ground waves also being used by some forces [1]. VHF/UHF links are not reliable to deal with beyond line-of-sight communication requirements. UHF is limited to line-of-sight and can only operate successfully if visual contact has occurred. VHF, though better than UHF in this scenario, also suffers from screening difficulties. Therefore short-range sky waves become a reliable solution to overcome such problems [1].

For most of the 20th century, HF communication was widely used for long-range transmission and worldwide coverage. Satellite communication later merged as an alternative to HF communication and HF technology was then considered to be obsolete. However, later in satellite area, it became clear that satellites were not the panacea they first appeared to be. A major vulnerability of most satellite-based networks is the need for ground stations since the transmission is typically routed through these stations and does not directly come from the satellite. The communication between ground station and end-user therefore becomes the weakest link of a satellite-based network in a disaster scenario such as earthquake, hurricane, terrorist attacks etc. Even the satellites themselves are vulnerable to hostile attacks (e.g., electronic jamming, electromagnetic pulse interference, physical destruction by a missile). Furthermore, problems with indoor reception, requirement for an unobstructed view of the satellite, high investment and maintenance costs make satellite communication less attractive for many purposes. With its enduring qualities, HF communication survived through this

competition and new generations of HF systems were introduced following the advances in DSP and VLSI technologies [1].

HF communication systems operate in a decentralized manner and are independent of a fixed infrastructure. This makes them particularly valuable in emergency and crisis situations such as earthquakes, floods, hurricanes, fires, political unrest, peace-keeping, and law-enforcement operations. A recent tragic example of the HF deployment efficiency in disaster situations was witnessed after Hurricane Katrina which caused devastation along much of the north-central of United States in 2005. With nearly all the high-end emergency communications gear, 911 call centers, cell phone towers and fixed phone lines being knocked out by the hurricane in its path, HF radio operators became a critical player in rescue and recovery operations [5]. The Red Cross issued a request for about 500 amateur radio operators and deployed them at the shelters it erected in the area. The members of American Radio Relay League (a national association of amateur radio operators) assisted first responders in search-and-rescue missions. Subsequent American congressional hearings highlighted the amateur radio response as one of the few examples of what went right in the disaster relief effort [6]. Such tragic incidents have resulted in re-appreciation of HF communication and would hopefully attract further interest into this technology.

Chapter 2

Fading Mitigation in HF Channel

2.1 Fading Channel Model for HF Propagation

As earlier described in Chapter 1, the propagation mechanism which allows long-distance, also known as over-the-horizon (OTH), transmission in HF band is sky wave propagation relying upon the refraction of the signals by the earth's ionosphere. The transmitted HF signal usually travels over several paths to the receiver via single and multiple reflections from the E and F layers of the ionosphere. This results in a multipath propagation where the delay spread is on the order of several milliseconds. As an example, Figure 2.1 illustrates the received multipath components if a continuous wave signal is transmitted over an HF link. In this figure, four paths are present; namely, one-hop E mode (1E), one-hop F mode (1F), two-hop F mode (2F), and a mixed mode (e.g., 1E + 1F).

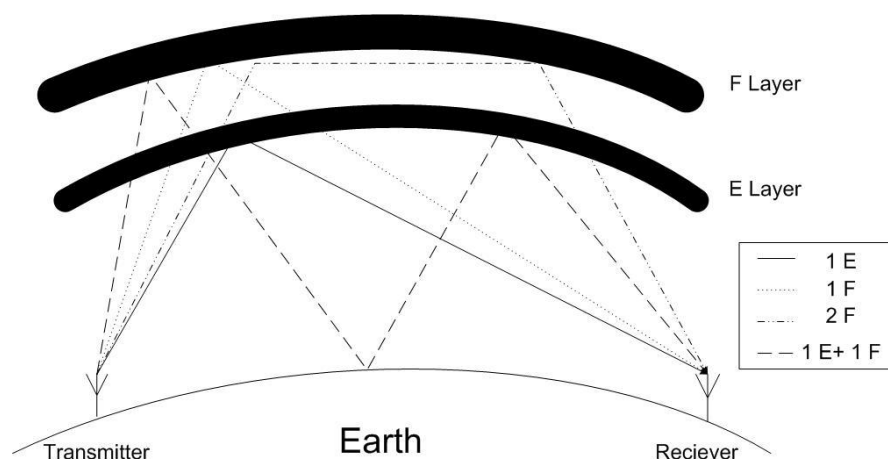


Figure 2.1: HF Radio Wave Propagation Modes

Besides the frequency-selectivity (i.e., temporal spread) introduced by the multipath propagation, the received signal is also subject to time-selectivity due to the changes and

movements in ionosphere. The temporal variations in the heights of ionospheric layers and electron density (and hence refractive index) along the paths induce Doppler spreads which are in the range of 0.1-1Hz for mid-latitudes, 0.5-10Hz for low-latitudes, and 0.5-30 Hz for high-latitudes [7]. Additional Doppler effects can be further present due to the speed of the mobile units in mobile HF applications.

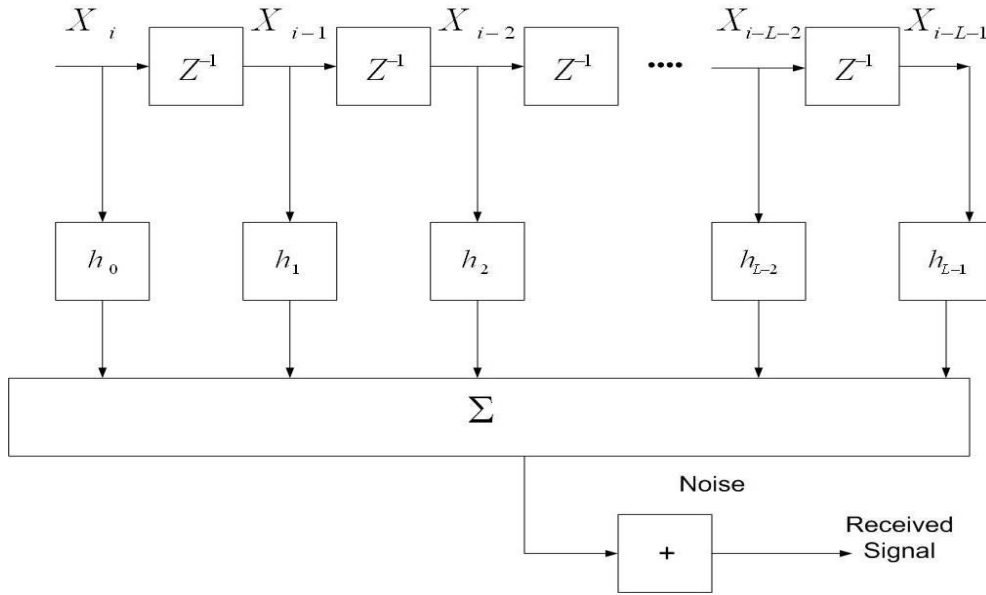


Figure 2.2: Watterson HF Tapped Line Model

The widely adopted channel model for HF ionospheric transmission is Watterson model [8, 9, 10] which is based on a tapped delay-line (See Figure 2.2) with L taps where each tap gain is given by

$$h_i(t) = G_{ia}(t) \exp(j2\pi f_{ia}t) + G_{ib}(t) \exp(j2\pi f_{ib}t) \quad (2.1)$$

where $G_{ia}(t)$ and $G_{ib}(t)$ are sample functions of two independent complex Gaussian ergodic random processes, each with zero mean values and independent real and imaginary components with equal root mean square (r.m.s) values. The subscripts a and b identify the two magneto-ionic components that can be present in each path. f_{ia} and f_{ib} represent the corresponding

frequency (Doppler) shifts at each tap which are related to the movement of the mobile terminal.

The power spectrum of each tap gain follows

$$H(f) = \frac{G_{ia}}{\sigma_{ia}\sqrt{2\pi}} \exp\left[-\frac{(f-f_{ia})^2}{2\sigma_{ia}^2}\right] + \frac{G_{ib}}{\sigma_{ib}\sqrt{2\pi}} \exp\left[-\frac{(f-f_{ib})^2}{2\sigma_{ib}^2}\right] \quad (2.2)$$

where σ_{ia} and σ_{ib} represent the Doppler spreads which are related to the movements in the ionospheric layers. This double-Gaussian spectrum (i.e., addition of two Gaussian spectrums) reduces to a single-Gaussian form if the Doppler shifts and spreads of the two magneto-ionic components are nearly equal.

Figure (2.3) shows the power spectrum of the two magneto-ionic components given by (2.2). The six parameters in (2.2) are taken from the experiment conducted by Watterson on November 30 1967 from 11:10 am- 11:20 am. It is observed that the power spectrum of Watterson model follows bi-Gaussian distribution with the present of the two magneto-ionic components.

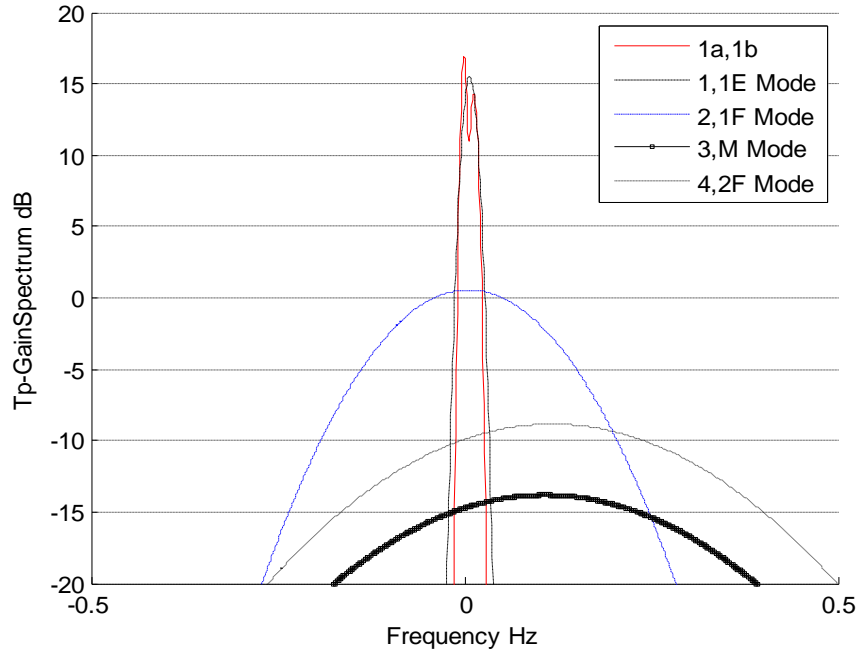


Figure 2.3: Tap Gain Spectrum for different HF modes

Based on Watterson’s tapped delay-line model, the received signal at signaling interval i can be given as

$$y_i = \sum_{j=0}^L h_j x_{i-j} + n_i \quad (2.3)$$

where h_j ($j = 0, 1, \dots, L$) are fading coefficients described by (2.1), x_i is the modulation signal and n_i is Additive White Gaussian noise (AWGN).

The International Radio Consultative Committee (CCIR) Recommendation [9] lists a number of HF channel conditions. They are defined as “Poor”, “Moderate” and “Good” channels. Each is described with their values of differential time delay and frequency spread for different latitudes as shown in Table 2.1.

	Low Latitude			Mid Latitude			High Latitude		
	Poor	Moderate	Good	Poor	Moderate	Good	Poor	Moderate	Good
Differential time delay τ	6	2	0.5	2	1	0.5	7	3	1
Frequency Spread σ_i	10	1.5	0.5	1	0.5	0.1	30	10	0.5

Table 2.1: Poor, moderate and good HF channels [9]

2.2 Diversity Techniques

The characteristics of ionospheric channel impose fundamental limitations on the performance of HF communication systems. The major impairment is fading which results in random fluctuations in the received signal level and affects the instantaneous signal-to-noise ratio (SNR). This requires the deployment of powerful diversity techniques to mitigate the

degrading effects of fading on the performance. Diversity improves the transmission performance by making use of more than one faded version of the transmitted signal. This improvement can be traditionally achieved exploiting time, frequency, space and/or polarization diversity. In the sections below, we discuss these types of diversity in the context of HF communications.

2.2.1 Frequency Diversity

This type of diversity is obtained by sending the same signal over different frequency carriers. Those frequencies should be separated sufficiently enough to guarantee uncorrelated fading. This might be practically hard to implement because of the requirement for multiple frequencies, which is not a bandwidth-efficient solution. In HF band, one may implement frequency diversity employing narrow frequency spacing (approximately less than 400 Hz) [1] tolerating some correlation.

2.2.2 Time Diversity

In this type of diversity, the same signal, or parts of it, is repeated in different time slots separated by an interval longer than the coherence time of the channel. Approximately a separation of 100 ms was found to be suitable to overcome fast, deep fades which makes received signal over the HF channel hard to decode [1]. Coding is a sophisticated way to exploit time diversity. In this technique, a codeword is sent instead of repeating sending the message. This allows not only the receiver system to determine that an error has occurred but also where it has occurred.

2.2.3 Space (Antenna) Diversity

In this type of diversity the transmitter and/or the receiver use multiple antennas. This technique does not require extra bandwidth. However, in order to ensure full diversity gain, sufficient separation between the antennas must be wide enough with respect to the wavelength. In HF communications, the carrier frequency is in the range of (2-30 MHz) that requires antenna

spacing to be several hundred meters (more than 500 m). This limits the use of space diversity for most practical purposes.

2.2.4 Polarization Diversity

This type of diversity is obtained by transmitting and receiving the same information signal simultaneously on orthogonally polarized waves. Polarization diversity gives the same performance as the antenna diversity with space and cost savings. However, there are some practical problems that must be taken in consideration in the application of polarization diversity in the HF channel. One can use vertical polarization to permit ground wave operation, or use horizontal polarization to help rejecting man-made noise and ground wave interferences. From a propagation point of view, both polarization are acceptable however there might be constraints related to the required radiation pattern, which are difficult to obtain with one or more polarizations.

2.3 Cooperative Diversity

Cooperative diversity has been recently proposed as a powerful alternative to antenna diversity. Cooperative diversity (also known as user cooperation) exploits the broadcast nature of wireless transmission and creates a virtual (distributed) antenna array through cooperating nodes to extract spatial diversity advantage.

The concept of cooperative diversity can be traced back to the work of Meulen [11] where he has analyzed a three-terminal relay network and introduced a two-hop communication system instead of point-to-point communication between source and destination. In [12], considering AWGN channels, Cover and Gamal have developed upper and lower bounds on capacity for a single-relay system. In [13] and [14], Sendonaris et al. have generalized the work of [15] for fading channels and shown that cooperating nodes in a wireless network provide higher data rates. Laneman et al. [15], [16] have proposed a cooperation protocol built upon a two-phase transmission scheme and demonstrated that the receiver can achieve full diversity by user cooperation. The work in [15] considers so-called Amplify-and-Forward (AaF) and Decode-and-

Forward (DaF) relaying techniques. These techniques differ from each other on how the received signal is processed at the relay station before it is sent to the destination. In DaF relaying, the relay terminal decodes the source node's message and then re-encodes it before transmitting to the destination. On the other hand, in AaF relaying, the relay amplifies and retransmits its received noisy signal without decoding it. Although the noise of the partner is amplified in this scheme, the destination still receives independently faded versions of the signal. In [17], Laneman et al. have applied conventional space-time codes to user cooperation systems in a distributed manner. Their proposed use of space-time block codes (STBCs) implements coding across the relay nodes assuming a scenario with more than one relay. Considering a single relay scenario, Nabar et al. [18] have also studied distributed STBC; however their setup realizes coding across the source and the relay nodes. Particularly, they consider the three following cooperation protocols.

Protocol I: In the first transmission phase (broadcasting phase), the source terminal broadcasts to the relay and destination terminals. During the second transmission phase (relaying phase), both the relay and source terminals communicate with the destination terminal. Protocol I in conjunction with AaF relaying is referred as “Non Orthogonal Amplify and Forward (NAF) protocol” in [19].

Protocol II: The source terminal communicates with the relay and destination terminals in broadcasting phase. In the relaying phase, the source stops transmission and only the relay terminal communicates with the destination. This protocol is the same as proposed in [15] and also referred as “Orthogonal Amplify and Forward (OAF) protocol” in [19].

Protocol III: This is similar to Protocol I except that the destination terminal does not receive from the source during the first transmission phase for reasons which are possibly imposed from the upper-layer networking protocols. For example, the destination terminal may be engaged in data transmission to another terminal during the first phase.

In Protocol II, the signal conveyed to the relay and destination terminals over the two phases is the same and Protocol II, therefore, effectively realizes receive diversity in a distributed manner. On the other hand, both Protocol I and Protocol III can potentially convey different signals to the relay and destination terminals. This makes possible the deployment of various conventional space-time codes (originally proposed for co-located antennas) in a distributed scenario. The table below summaries these three protocols

Time slot/ Protocol	I	II	III
1	$S \rightarrow R, D$	$S \rightarrow R, D$	$S \rightarrow R$
2	$S \rightarrow D, R \rightarrow D$	$R \rightarrow D$	$S \rightarrow D, R \rightarrow D$

Table 2.2: Cooperation protocols for a single-relay network where source, relay and destination terminals are denoted by S, R and D.

2.4 Motivation and Thesis Objective

Within the last decade, we have witnessed exciting developments in the area of communication theory; most notably MIMO (multiple-input multiple-output) and cooperative communication techniques. Neither MIMO nor cooperative communication has been extensively investigated for HF band with a few recent exceptions [20, 21]. Being cautious on the concept of MIMO HF is understandable because the separation between antennas to extract diversity is of the order of several hundred meters considering that the wavelengths in HF band are in the range of 10m-150m. This limits the potential use of MIMO HF for certain fixed applications where deployment area of HF station permits such wide uses of space. On the other hand, cooperative communication is an effective means to exploit the spatial dimension of the wireless channel in HF band. An initial performance study of a cooperative HF system by Cornell University for a US Navy project has already demonstrated the potential of this emerging concept [21]. This

study is basically limited to a quasi-static channel assumption and furthermore assumes perfect channel state information. Our study aims to provide better insight into system performance of a cooperative HF system encoupled with OFDM (orthogonal frequency division multiplexing) and pilot-assisted channel estimation over doubly-selective channels.

Orthogonal frequency division multiplexing (OFDM) was first introduced three decades ago. The basic concept of OFDM is to transmit multiple signals simultaneously over a single transmission path, where the signal travels within a given carrier. OFDM has become increasingly popular nowadays as effective multi-carrier transmission technique over frequency-selective channels. OFDM transforms frequency-selective channels into parallel flat fading channels that lead to design of the receiver with less complexity. However, the price paid is that no full diversity is achieved in uncoded OFDM due to the fact that each symbol is transmitted over a single frequency-flat fading channel. To achieve full diversity gain, coded OFDM has been introduced [22]. Linear constellation pre-coding OFDM (LCP-OFDM) proposed in [23] is another effective technique of achieving optimal diversity gain for coded OFDM over multi-path channels. It does not reduce the transmission rate of the uncoded OFDM and guarantees low complexity at the receiver side.

Since HF channel is subject to time-selectivity, efficient channel estimation is crucial to maintain a good performance. In coherent detection, the fading channel coefficients are estimated and then used in the detection process. The quality of channel estimates thus affects the overall system performance and might become a performance limiting factor particularly for time-selective channels. In general, channel fading coefficients can be acquired by either blind techniques or through the use of pilot symbols. In practical implementation, blind estimation techniques suffer from high complexity and identification ambiguities as well as slow convergence properties which are particularly prohibitive for high-mobility vehicular scenarios. On the other hand, pilot assisted channel estimation (PACE) techniques rely on the insertion of known training (pilot) symbols in information-bearing data. These pilot symbols and the specific multiplexing scheme are known at the receiver and can be exploited for channel estimation and

tracking purposes. PACE simplifies the challenging task of receiver design for unknown channels [24].

The rest of the thesis is organized as follows: In Chapter 3, we introduce the cooperative OFDM system model under consideration and present extensive simulation results over HF channels for various propagation conditions. The conclusions are provided in Chapter 4.

Chapter 3

Cooperative OFDM for HF Communications

There is an increasing demand for higher data speeds in HF communication systems. Current HF communication systems are not used only for the traditional voice transmission, but also for data communication (including file transfer, facsimile, e-mail, internet access), still-image transmission and even for real-time video conferencing [25, 26]. The data rates that can be supported by the currently available HF single-carrier transceivers with 3 kHz bandwidth are typically limited to 9.6 kbps (kilobits per second). Targeting data rates of several tens of kbps over an HF channel with typical delay spreads on the order of several milliseconds results in intersymbol interference (ISI) spanning tens, or even hundred of symbols. High-speed HF communication systems should be, therefore, designed to handle such severe ISI.

An efficient approach to mitigate ISI is OFDM (orthogonal frequency division multiplexing). OFDM has been already adopted by major manufacturers and by standardization bodies for a wide range of wireless applications in different parts of the electromagnetic spectrum. In HF band, OFDM has been the physical layer choice for the new digital broadcasting system known as Digital Radio Mondiale (DRM) which was introduced in 2003 [27]. Furthermore, the current military HF standards also support multi-carrier communication as a non-mandatory option. It has been also recently discussed within the amateur radio community if a new OFDM-based standard should be adopted [28]. The current trends indicate that most of the next-generation HF systems would likely build on a multi-carrier physical layer which is also considered in this thesis.

OFDM is an effective method to mitigate the degrading effect of the ISI resulting from frequency selectivity of the HF channel by converting the time-domain channel into a set of scalar channels in the frequency domain. There are three main steps involved: First, the transmitted data is divided into parallel blocks (subcarriers) instead of transmitting it as a serial stream. Those carriers are separated in a smart manner to ensure the orthogonality. This blocks the demodulators from seeing frequencies other than their own, and as a result subcarriers will

not interfere with each other as they are sampled at the subcarrier frequencies. Then, a Fourier transform is applied to the data in each OFDM block. Finally, to recover inter-block interference effect a cyclically extended guard interval is inserted prior to each OFDM block. The length of the guard interval is equal to or larger than the number of channel taps.

3.1 Transmission Model

In this thesis, we investigate an OFDM cooperative communication system over HF channel assuming amplify-and-forward (AaF) relaying. We consider a single-relay scenario where source node S, relay node R, and destination node D operate in half-duplex mode as illustrated in Figure 3.1. A single pair of transmit and receive antennas is employed at each terminal.

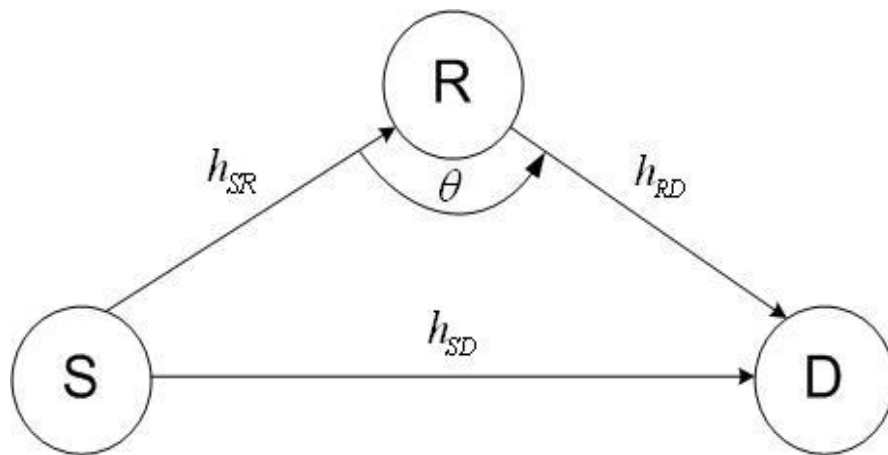


Figure 3.1 Single-relay network.

We consider an aggregate channel model which takes into consideration both long-term path loss and short-term fading. The path loss between any two nodes is proportional to $d^{-\alpha}$ where d is the propagation distance and α is the path loss coefficient. The path loss between nodes A and B is given by

$$Loss(A, B) = \frac{k}{d_{AB}^{\alpha}} \quad (3.1)$$

where k is the constant depending on propagation environment, d_{AB} is the Euclidean distance between the two nodes. We set the path loss in source-to-destination S→D link to be unity, therefore the relative geometrical gain of source-to-relay S→R and relay-to-destination R→D links are, respectively, defined as

$$G_{SR} = \frac{Loss_{S,R}}{Loss_{S,D}} = \left(\frac{d_{SD}}{d_{SR}} \right)^\alpha \quad (3.2)$$

$$G_{RD} = \frac{Loss_{R,D}}{Loss_{S,D}} = \left(\frac{d_{SD}}{d_{RD}} \right)^\alpha \quad (3.3)$$

which are related to each other through cosine theorem as

$$G_{SR}^{-2/a} + G_{RD}^{-2/a} - 2G_{SR}^{-1/a}G_{RD}^{-1/a} \cos \theta = 1 \quad (3.4)$$

where θ is the angle between links S→R and R→D. We further define β as

$$\beta = \frac{G_{SR}}{G_{RD}} = \left(\frac{d_{RD}}{d_{SR}} \right)^\alpha \quad (3.5)$$

The more negative this ratio is (given in dB), more close the relay is located to the destination. On the other hand, positive values indicate the relay and source are closer. The particular case of the $\beta = 0$ dB means that both source and destination terminals have same distance to the relay.

G_{SR} and G_{RD} can be further rewritten in terms of β as

$$G_{SR} = 1 + \beta - 2\sqrt{\beta} \cos \theta \quad (3.6)$$

$$G_{RD} = \frac{1 + \beta - 2\sqrt{\beta} \cos \theta}{\beta} \quad (3.7)$$

The channel impulse responses (CIRs) for S→D, S→R and R→D are given by

$$\mathbf{h}_{SR} = [h_{SR}(0), h_{SR}(1), \dots, h_{SR}(L_{SR})]$$

$$\mathbf{h}_{RD} = [h_{RD}(0), h_{RD}(1), \dots, h_{RD}(L_{RD})]$$

$$\mathbf{h}_{SD} = [h_{SD}(0), h_{SD}(1), \dots, h_{SD}(L_{SD})]$$

where each tap is modeled by (2.2) following Watterson HF channel model. \mathbf{h}_{SR} , \mathbf{h}_{SD} and \mathbf{h}_{RD} are assumed to be identically independent and they remain constant over a period of one block transmission and vary independently from block to another.

We consider Protocol II with AaF relaying. In the broadcasting phase, the source node transmits to both the destination node and relay node. In the relaying phase, the source node is silent and only the relay node forwards its received signal to the destination node. Our system is built on OFDM transmission with linear constellation precoding. Let \mathbf{s} denote the two dimensional transmitted information data block of size $N \times T$ where N is the number of subcarriers in frequency domain and T is the number of OFDM blocks in time domain. Pilot symbols are inserted periodically with equal spacing in both time and frequency domains to help estimating the channel as illustrated in Figure (3.2).

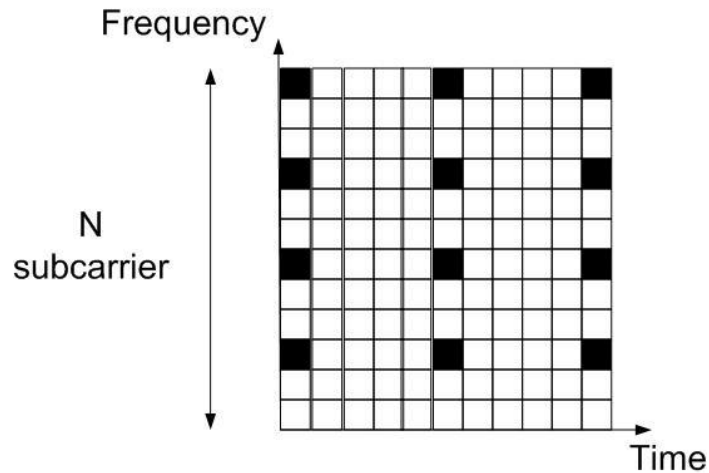


Figure 3.2 Frame structure for OFDM with pilot symbols inserted in time and frequency domains.

The precoded data is written as $\mathbf{x} = \Theta \mathbf{s}$ where Θ is the precoded matrix of size $N \times N$ defined as

$$\Theta = \frac{1}{\sqrt{\beta_{\Theta}}} \begin{bmatrix} 1 & \alpha_{\Theta 1} & \cdots & \alpha_{\Theta 1}^{L-1} \\ 1 & \alpha_{\Theta 2} & \cdots & \alpha_{\Theta 2}^{L-1} \\ 1 & \vdots & \cdots & \vdots \\ 1 & \alpha_{\Theta L} & \cdots & \alpha_{\Theta L}^{L-1} \end{bmatrix} \quad (3.8)$$

satisfying power constraint $\text{tr } \Theta \Theta^H = N$. Here, β_{Θ} is a normalization factor equal to the number of taps $L = \max L_{SR}, L_{SD}, L_{RD}$ where L_{SR} , L_{SD} and L_{RD} are number of taps of S→R, S→D and R→D links, respectively, and α_{Θ} is a parameter which depends on L , see Table 3.1.

	α_1	α_2	α_3	α_4	α_5	α_6	α_7	α_8
	$e^{-j\frac{\pi}{4}}$	$e^{-j\frac{5\pi}{4}}$						
	$\sqrt[3]{2}e^{-j\frac{\pi}{12}}$	$\sqrt[3]{2}e^{-j\frac{9\pi}{12}}$	$\sqrt[3]{2}e^{-j\frac{17\pi}{12}}$					
	$e^{-j\frac{\pi}{8}}$	$e^{-j\frac{5\pi}{8}}$	$e^{-j\frac{9\pi}{8}}$	$e^{-j\frac{13\pi}{8}}$				
	$\sqrt[5]{2}e^{-j\frac{\pi}{20}}$	$\sqrt[5]{2}e^{-j\frac{9\pi}{20}}$	$\sqrt[5]{2}e^{-j\frac{17\pi}{20}}$	$\sqrt[5]{2}e^{-j\frac{25\pi}{20}}$	$\sqrt[5]{2}e^{-j\frac{33\pi}{20}}$			
	$e^{-j\frac{2\pi}{7}}$	$e^{-j\frac{4\pi}{7}}$	$e^{-j\frac{6\pi}{7}}$	$e^{-j\frac{8\pi}{7}}$	$e^{-j\frac{10\pi}{7}}$	$e^{-j\frac{12\pi}{7}}$		
	$\sqrt[7]{2}e^{-j\frac{\pi}{28}}$	$\sqrt[7]{2}e^{-j\frac{9\pi}{28}}$	$\sqrt[7]{2}e^{-j\frac{17\pi}{28}}$	$\sqrt[7]{2}e^{-j\frac{25\pi}{28}}$	$\sqrt[7]{2}e^{-j\frac{33\pi}{28}}$	$\sqrt[7]{2}e^{-j\frac{41\pi}{28}}$	$\sqrt[7]{2}e^{-j\frac{49\pi}{28}}$	
	$e^{-j\frac{\pi}{16}}$	$e^{-j\frac{5\pi}{16}}$	$e^{-j\frac{9\pi}{16}}$	$e^{-j\frac{13\pi}{16}}$	$e^{-j\frac{17\pi}{16}}$	$e^{-j\frac{21\pi}{16}}$	$e^{-j\frac{25\pi}{16}}$	$e^{-j\frac{29\pi}{16}}$

Table 3.1: Parameter α for different values of L

After applying the Inverse Fast Fourier Transform (IFFT) on \mathbf{x} , a cyclic prefix of length is added between adjacent information data block to avoid inter-block interference. Since each symbol is transmitted over all the sub-carriers in OFDM, decoder complexity can be prohibitive. To reduce decoding complexity, we adopt sub-carrier grouping technique [23]. Here we assume the subcarriers are grouped into M groups each of which consists of $L+1$ subcarriers, which is equal to the channel length. Therefore, $N=(L+1)M$ is the total number of subcarrier and is the length of a single data OFDM block.

FFT is only performed at the destination, not at the relay terminal. After removing cyclic prefix, the received data at the relay node is given by

$$\mathbf{r}_{SR} = \sqrt{G_{SR}E} \mathbf{H}_{SR} \mathbf{Q}^H \mathbf{x} + \mathbf{n}_R \quad (3.9)$$

where E is the average power, \mathbf{H}_{SR} is a $N \times N$ circulant matrix of the S \rightarrow R channel with entries of \mathbf{H}_{SR} $p, q = (\mathbf{h}_{SR}(p-q) \bmod N)$, $p, q = 1, 2, \dots, N$ and \mathbf{n}_R is additive white Gaussian noise of size $N \times T$ at the relay node with zero mean and covariance matrix $N_0 \mathbf{I}_N$. The relay node normalizes the respective received signal \mathbf{r}_R by a factor of $\sqrt{E \|\mathbf{r}_R\|^2}$ to ensure the unity of average of energy and then re-transmits the signal to the destination during the second time slot.

The received signal at destination during the broadcasting and relaying phase are given by

$$\mathbf{r}_{D1} = \sqrt{E} \mathbf{Q} \mathbf{H}_{SD} \mathbf{Q}^H \mathbf{x} + \mathbf{n}_{D1} \quad (3.10)$$

$$\mathbf{r}_{D2} = \sqrt{G_{RD}E} \mathbf{Q} \mathbf{H}_{RD} \mathbf{Q}^H \frac{\mathbf{r}_R}{\sqrt{E \left(\|\mathbf{r}_R\|^2 \right)}} \mathbf{x} + \mathbf{n}_{RD} \quad (3.11)$$

$$= \sqrt{\frac{G_{RD}E}{G_{SR}E + N_0}} \sqrt{G_{SR}E} \mathbf{Q} \mathbf{H}_{RD} \mathbf{H}_{SR} \mathbf{Q}^H \mathbf{x} + \tilde{\mathbf{n}}_{RD} \quad (3.12)$$

where \mathbf{H}_{SD} and \mathbf{H}_{RD} are $N \times N$ circulant matrix of the S \rightarrow D and R \rightarrow D channels with entries of \mathbf{H}_{SD} $p, q = (\mathbf{h}_{SD}(p-q) \bmod N)$ and \mathbf{H}_{RD} $p, q = (\mathbf{h}_{RD}(p-q) \bmod N)$ respectively. $\tilde{\mathbf{n}}_{RD}$ in (3.12) is defined as $\tilde{\mathbf{n}}_{RD} = A \mathbf{H}_{RD} \mathbf{n}_{RD} + \mathbf{n}_{RD}$ and it is conditionally Gaussian (condition on \mathbf{H}_{RD}) with zero

mean and covariance matrix $N_0\Gamma$ where $\Gamma = (A^2\mathbf{D}_{RD}\mathbf{D}_{RD}^H + 1)\mathbf{I}_p$ and A is defined as $A = \sqrt{G_{RD}E/(G_{SR}E + N_0)}$.

Let $D(n) = \sum_{k=0}^L \mathbf{h}(k) \exp -j2\pi kn / N$, $n=1,2,\dots,N$ denote the frequency response evaluated at the FFT grid for a given link with CIR length $L+1$. It is easy to show that $\mathbf{D} = \mathbf{Q}\mathbf{H}\mathbf{Q}^H = \text{diag } D(0), D(1), \dots, D(N-1)$. This lets us to rewrite (3.10) and (3.12) as

$$\mathbf{r}_{D1} = \sqrt{E}\mathbf{D}_{SD}\mathbf{x} + \mathbf{n}_{D1} \quad (3.13)$$

$$\mathbf{r}_{D2} = A\sqrt{G_{SR}E}\mathbf{D}_{RD}\mathbf{D}_{SR}\mathbf{x} + \tilde{\mathbf{n}}_{RD} \quad (3.14)$$

Then, (3.13) and (3.14) can be written in a compact matrix form as

$$\mathbf{r} = \begin{bmatrix} \sqrt{G_{SD}E}\mathbf{D}_{SD} \\ \sqrt{G_{SR}E}A\Gamma^{-1/2}\mathbf{D}_{RD}\mathbf{D}_{SR} \end{bmatrix} \mathbf{x} + \mathbf{n} \quad (3.15)$$

where $\mathbf{r} = [r_{D1} \ \hat{r}_{D2}]^T$ and $\mathbf{n} = [n_{D1} \ \hat{n}_{D2}]^T$. This is fed to the ML decoder given as

$$\arg \min_{\mathbf{x}} \|\mathbf{r} - \mathbf{x}\hat{\mathbf{H}}\|^2 \quad (3.16)$$

where $\hat{\mathbf{H}}$ is the channel estimate.

For channel estimation, we use PACE which relies on the insertion of known training (pilot) symbols in information-bearing data. In our simulations, we used Spline interpolation technique for estimating time-variant channel [24, 29]. Spline interpolation, or Cubic polynomial interpolation, is a powerful data analysis tool. Unlike Wiener interpolation, where certain data IS involved in the interpolation process depending on number of pilots used and interpolation size, it correlates data efficiently and effectively with using all the data in a given grid. In Spline interpolation, the relation between the estimated channel at a given subcarrier and the received signal at the pilot position in is given by

$$\hat{H}_{n,k} = \sum_{p=1}^{N_{pi}} r_{n,k} H_{n,p} \quad (3.17)$$

where N_{pf} is the number of pilot in the frequency domain, $r_{n,k}$ is the received signal at subcarrier k . and $H_{n,p}$ is the channel frequency response at the pilot location p .

3.2 Simulation Results and Discussion

In this section, we present Monte-Carlo simulation results to demonstrate the error rate performance of OFDM transmission technique over HF channel considering single-input-single-output (SISO) and AaF cooperative relaying. We consider three different HF channel types, poor, moderate and good using the values in Table 2.1 for high latitudes and assume both cases of perfect and imperfect channel state information (CSI). We assume BPSK modulation, $N = 26$ subcarriers with $N_{pf} = 6$ pilots and spacing $s_f = 5$ in the frequency domain. We assume number of frames in the time domain $T = 13$ with $N_{pt} = 4$ and spacing $s_t = 4$ with a varying number of pilot symbols. The gain values for both magnetoionic components are taken as $G_{ia} = G_{ib} = 0.5$, and frequency spread values under consideration are provided Table 2.1. As for the frequency shift in mobile HF applications, the Doppler shift is calculated as $f_d = v/\lambda$, where v is the mobile speed and $\lambda = c/f_c$ is the wavelength and $f_c = 2 - 30$ MHz is the upper and lower carrier frequencies in the HF band.

In figures (3.3) and (3.4), we illustrate the BER performance of the three HF channel types in SISO environment considering perfect CSI and estimated cases respectively. We observe from both figures that the Good channel outperforms the Moderate and the Poor channel by approximately 1.5 dB and 2 dB respectively. However, the difference between the Moderate and Poor channels is observed to be very small.

In figures (3.5) and (3.6), we investigate the effect of channel estimation assuming different mobility environments over the Good HF channel. Specifically, we consider six cases:

- 1) The mobile terminal is fixed ($f_{\text{shift}}=0$).
- 2) The mobile terminal moves at a speed of 60 km/h and operates over 2 MHz resulting in a frequency shift equal to 0.2 Hz

3) The mobile terminal moves at a speed of 60 km/h and operates over 30 MHz resulting in a frequency shift equal to 1.7 Hz.

4) Speed 100km/h and $f_{\text{shift}}=2.7\text{Hz}$.

5) Speed 120 km/h s and $f_{\text{shift}}=3.3\text{Hz}$.

6) Speed 140 km/h and $f_{\text{shift}}=3.8\text{Hz}$

It is observed that for fixed case there is a performance difference of 1.2dB between perfect and imperfect channel estimation. The performance gets worse as frequency shift is introduced. Specifically, ~ 1.5 dB degradation occurs when the frequency shift changes from 0 to 0.2 Hz. A performance degradation of 1 dB occurs as the frequency shift changes from 0.2 Hz to 1.7 Hz. When the speed of the mobile terminal further increases, an error floor occurs caused by the fact that the total bandwidth exceeds that of the interpolation size which depends on the number of pilots.

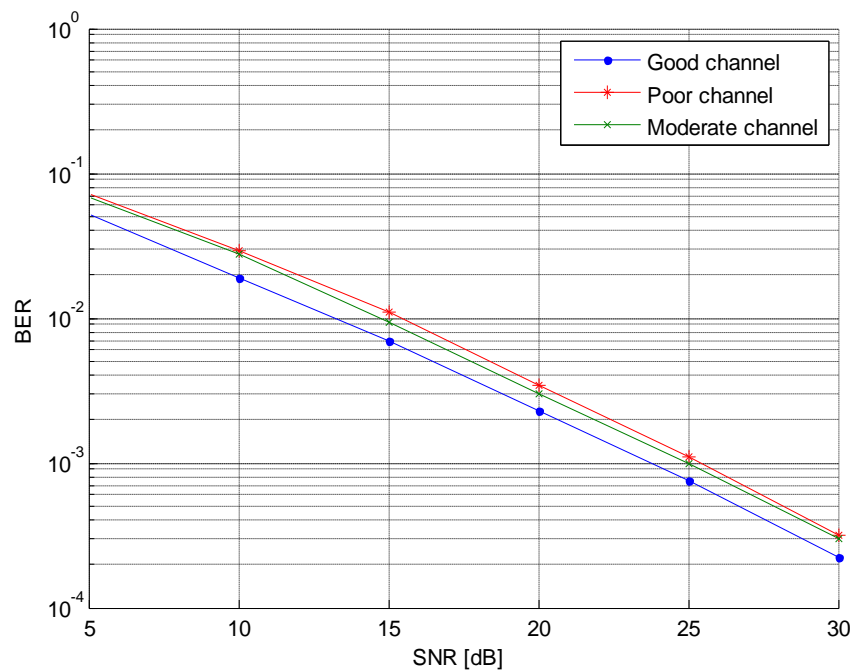


Figure 3.3 Performance of SISO OFDM over HF channels with perfect channel estimation.

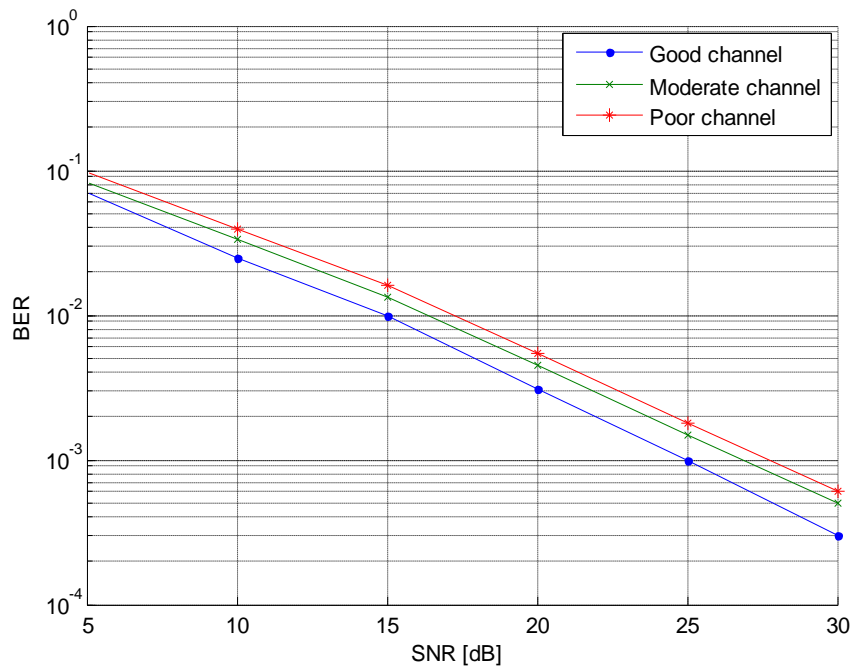


Figure 3.4 Performance of SISO OFDM over HF channels with imperfect channel estimation.

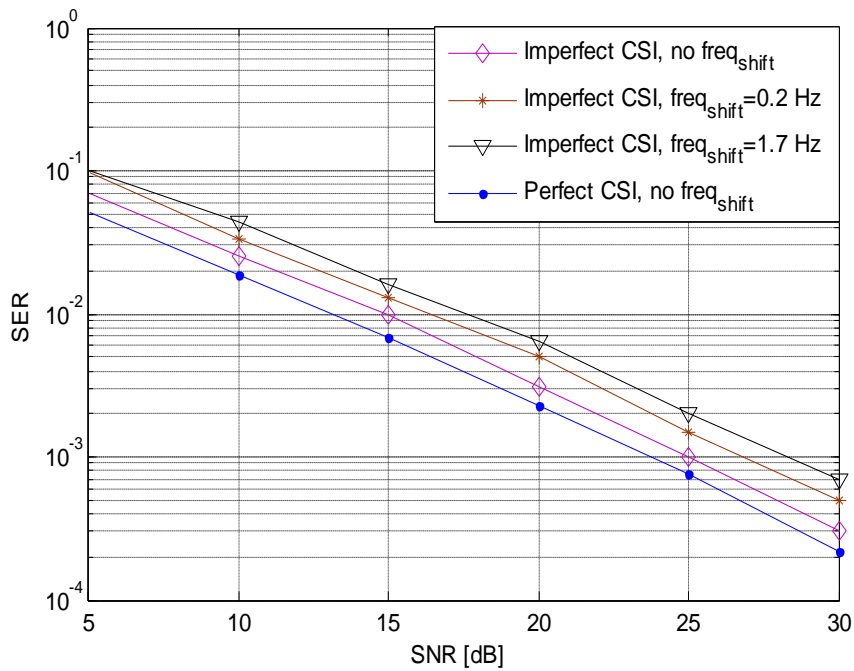


Figure 3.5: Effect of channel estimation on the performance of SISO OFDM for different Doppler shifts (Good HF channel)

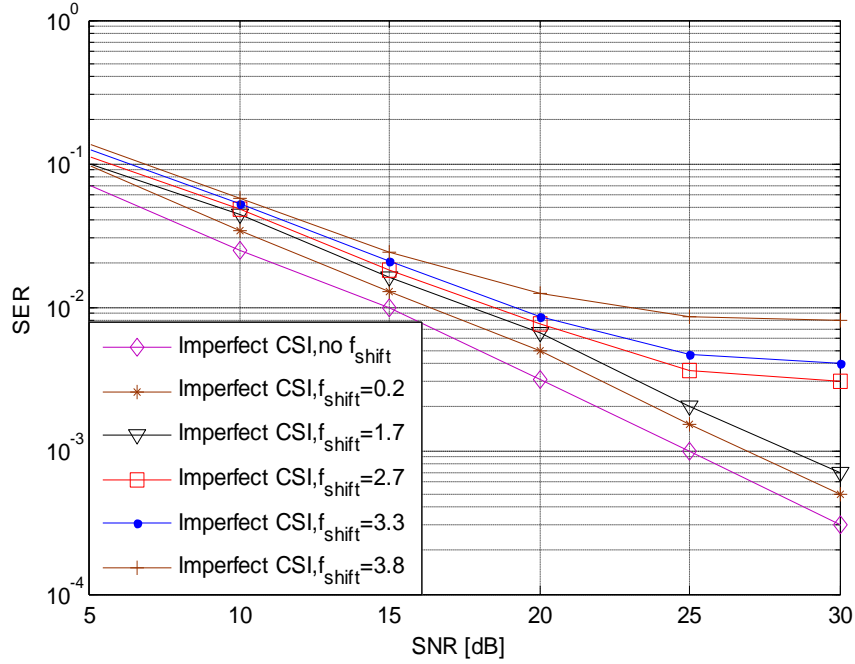


Figure 3.6 Effect of channel estimation on the performance of SISO OFDM for different Doppler shifts (Good HF channel).

In figures (3.7) and (3.8), we present the BER performance of the cooperative OFDM system over three HF channel types. We assume $\theta = \pi$ and $G_{SR}/G_{RD} = 0$ dB. The channel lengths L_{SR} , L_{SD} and L_{RD} are assumed to be equal to 2. We consider both uncoded and precoded OFDM. The uncoded OFDM is not able to exploit the underlying multipath diversity and its diversity order is limited to 2. On the other hand, precoded OFDM further takes advantages of the multipath diversity and extracts a diversity order of 4. Comparison of different channel types further reveals that the performance of the Good channel outperforms the Moderate and the Poor channel by approximately 2 dB and 2.5dB respectively.

In figure (3.9), we investigate the effect of different channel taps. We consider only the Good channel and assume the following two cases.

- 1) The channel memory lengths L_{SR} , L_{SD} and L_{RD} are equal to 2.

2) The channel memory lengths L_{SR} , L_{SD} and $L_{RD} = 3$.

Our results illustrate that the diversity orders are equal to 4 and 6, respectively, for the first and second cases similar to the earlier observations reported in [30] for cooperative OFDM systems over Rayleigh fading channels. It is also observed that there is a performance difference of approximate 4dB between perfect and imperfect channel estimation.

In figures (3.10) and (3.11), we further investigate the effect of channel estimation by changing the speed of the mobile terminal under the assumption of the Good HF channel. We consider the same scenarios earlier studied for SISO system. It is observed that the performance gets worse as frequency shift is introduced. Specifically, about 2 dB degradation occurs when the frequency shift changes from 0 to 0.2 Hz. A performance degradation of 1.2dB occurs as the frequency shift changes from 0.2 Hz to 1.7 Hz.

In figure (3.12), we investigate the effect of relay location on the performance of cooperative OFDM. We consider three cases:

- 1) $G_{SR}/G_{RD} = -30 \text{ dB}$ (i.e., the relay terminal is close to destination terminal)
- 2) $G_{SR}/G_{RD} = 0 \text{ dB}$ (i.e., the relay terminal is in the middle)
- 3) $G_{SR}/G_{RD} = 30 \text{ dB}$ (i.e., the relay terminal is close to source terminal).

The best performance is observed at -30 dB when the relay terminal is close to destination terminal. This is rather expected since Protocol II under consideration mimics receive diversity.

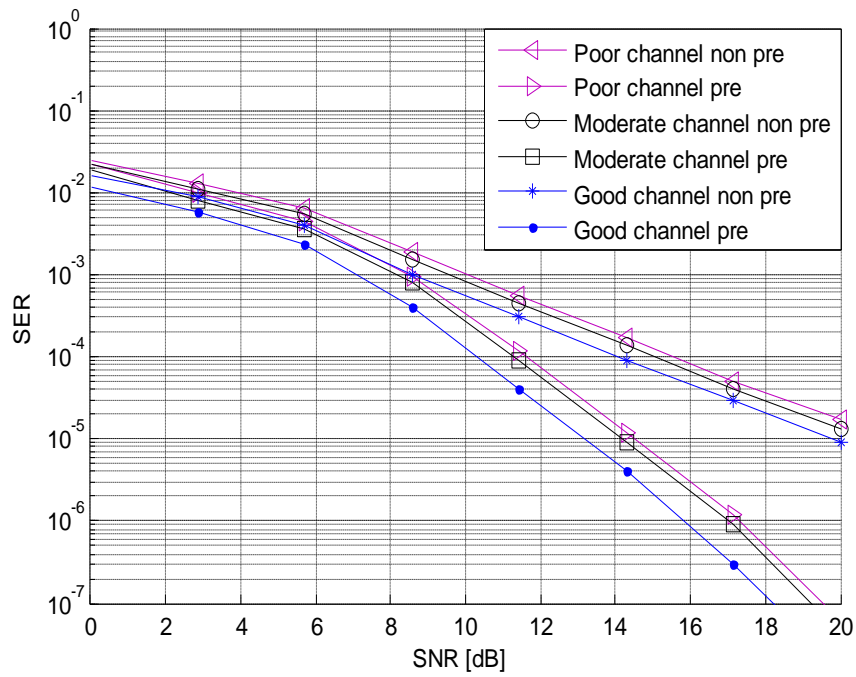


Figure 3.7 Performance of cooperative OFDM over HF channels with perfect channel estimation.

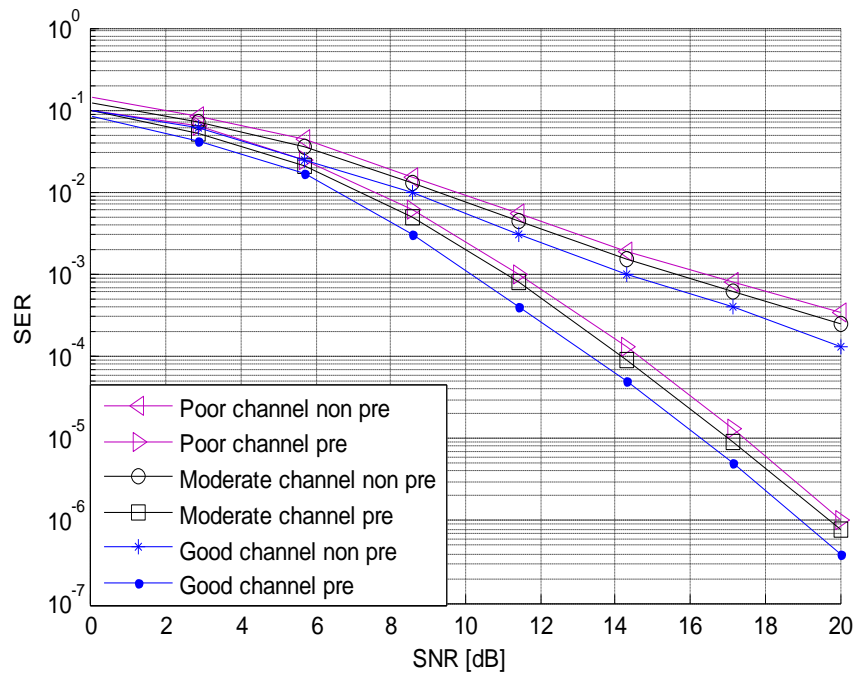


Figure 3.8 Performance of cooperative OFDM over HF channels with imperfect channel estimation.

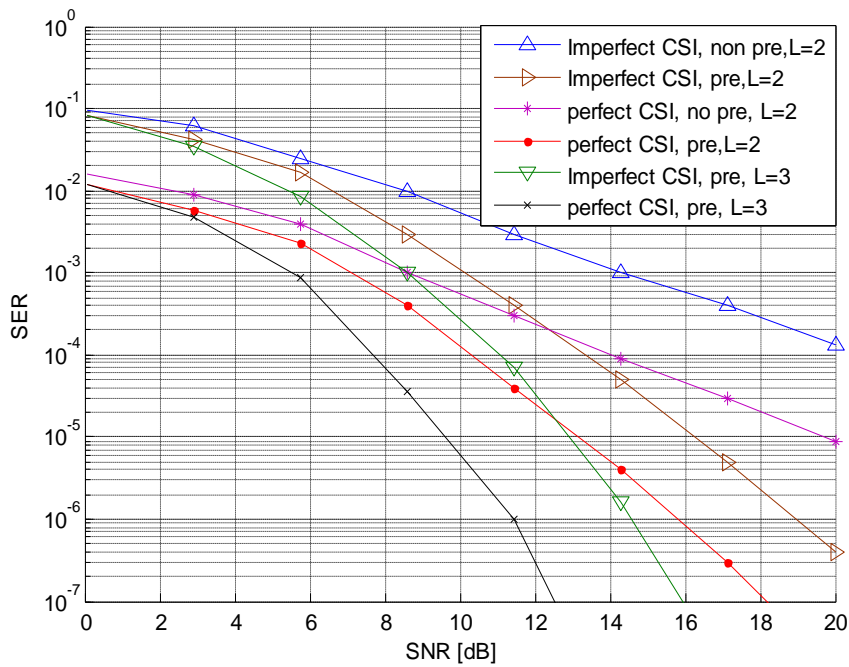


Figure 3.9 Effect of channel lengths on the performance of cooperative OFDM (Good HF channel)

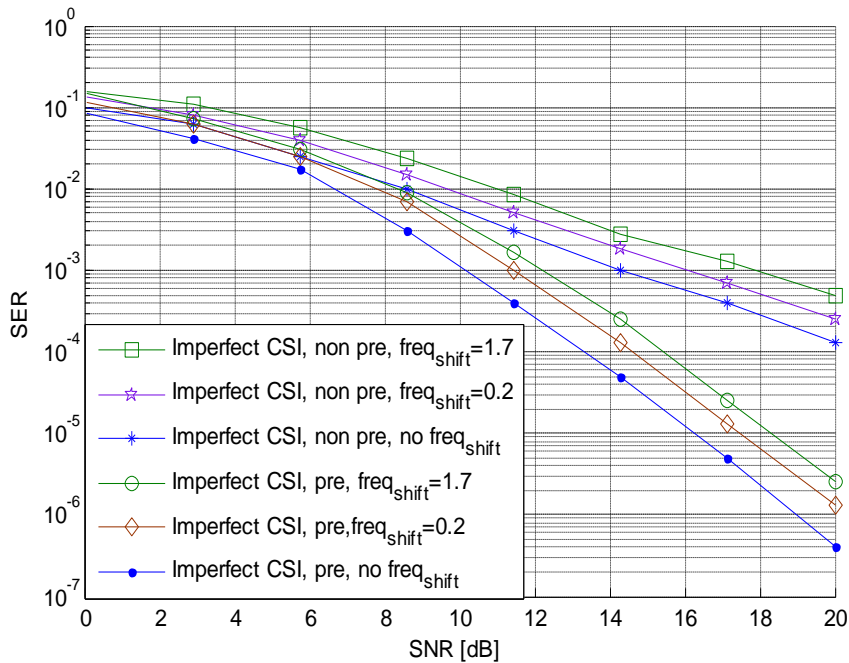


Figure 3.10 Effect of channel estimation on the performance of cooperative OFDM for different Doppler shifts (Good HF channel)

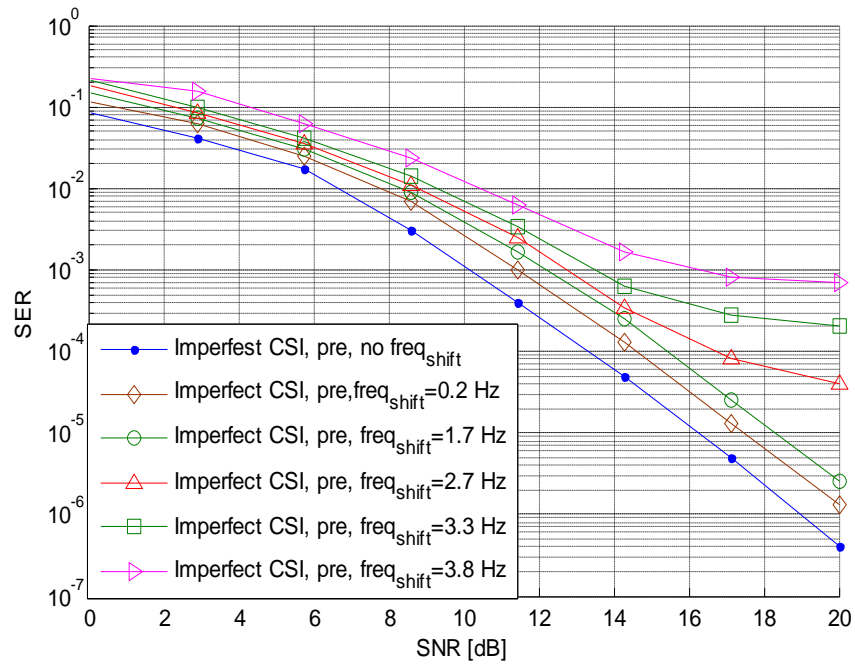


Figure 3.11 Effect of channel estimation on the performance of cooperative OFDM for different Doppler shifts (Good HF channel)

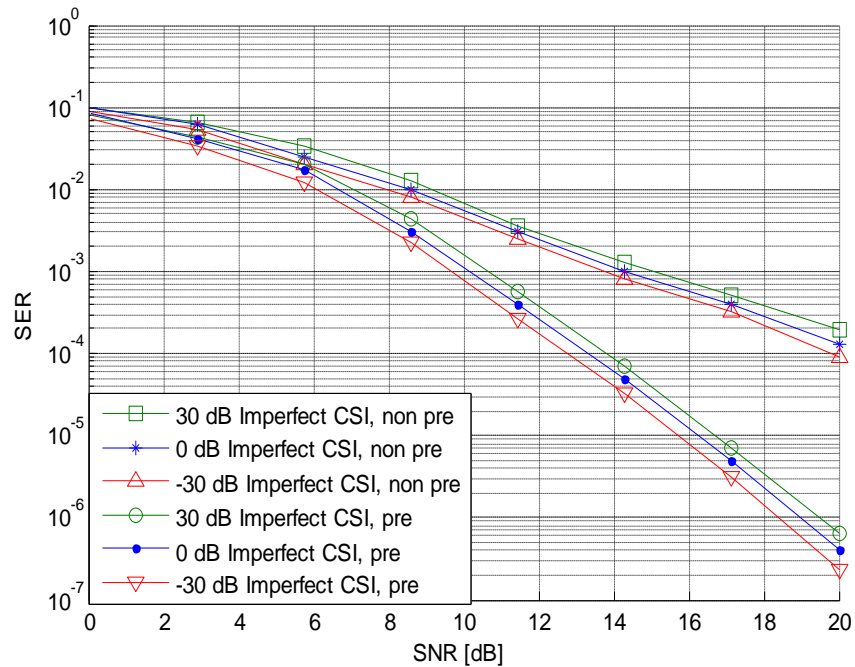


Figure 3.12 Effect of relay location on the performance of cooperative OFDM

Chapter 4

Conclusions

HF communication has been an essential part of worldwide information transmission since the advent of radio. For decades, HF band has been recognized as the primary means for long-range wireless communications. Satellite communication later merged as an alternative to HF communication and HF technology was then considered to be obsolete. With its enduring qualities, HF communication survived through this competition and new generations of HF systems were introduced following the advances in DSP and VLSI technologies.

With research efforts focusing on more profitable sectors of telecommunications, HF communication has received much less attention than it deserves. This might also come from the misleading perception that it is already a mature technology. On contrary, HF communication has evolved substantially in the last decade. Current HF communication systems are not used only for the traditional voice transmission, but also for data communication (including file transfer, facsimile, e-mail, internet access), still-image transmission and even for real-time video conferencing. Traditional analog voice transmission has been recently replaced by digital techniques as seen in the recent introduction of DRM broadcasting [3]. The shift from analog to digital in voice communications and demanding requirements of high-speed data communications impose new requirements on the HF system design some of which are addressed in this thesis.

Within the last decade, we have witnessed exciting developments in the area of communication theory; most notably MIMO (multiple-input multiple-output) and cooperative communication techniques. Building upon the promising combination of cooperative communication and HF transmission, this thesis has investigated the performance of a cooperative OFDM system over HF channels under various propagation environments. Specifically, we investigated the performance of cooperative OFDM for so-called Good, Moderate and Poor HF Channels through an extensive Monte-Carlo simulation. We studied both perfect and imperfect channel estimation. The imperfect channel estimation results in some

performance degradation, but does not affect the diversity order. These results clearly indicate that cooperative transmission is a suitable diversity technique for HF communication in which multiple antenna deployment is not possible due to the excessive space requirements.

Bibliography

- [1] N. M. Maslin, HF Communications: A System Approach, *Pitman Publishing*, London, 1987.
- [2] K. Davies, *Ionospheric Radio Waves*, *Blaisdell Publishing Company*, USA, 1969.
- [3] J. Lavergnat and M. Sylvain, Radio Wave Propagation: Principle and Techniques, *John Wiley & Sons, Ltd.* England, 2000.
- [4] <http://www.weather.nps.navy.mil>
- [5] I. Urbina, Lacking Phone Lines, Rescues Turn to Ham Radio Operators, *New York Times*, Sept. 8, 2005.
- [6] F. F. Townsend, The Federal Response to Hurricane Katrina: Lessons Learned, *The White House Report*, Washington DC, Feb. 2006.
- [7] “Testing of HF Modems with Bandwidths of up to about 12 KHz using Ionospheric Channel Simulators,” *ITU-R F.1487 Recommendation*, 2000.
- [8] W. N. Furman and J. W. Nieto, “Understanding HF Channel Simulator Requirements in order to Reduce HF Modem Performance Measurement Variability,” *Harris Corporation, RF Communications Division*.
- [9] ITU, Recommendation 520-1 “Use of High Frequency Ionospheric Channel Simulators,” *Recommendations and Reports of the CCIR*, vol. III, p. 57-58, 2000.
- [10] C. C. Watterson, J. R. Juroshek and W. D. Bensema, “Experimental Confirmation of an HF Channel Model,” *IEEE Trans. on Comm. Tech.*, vol. COM-18, no.6, Dec. 1970.
- [11] E. V. D. Meulen, “Three-terminal communication channels,” *Advances in Applied Probability*, vol. 3, p. 120-154, 1971.
- [12] T. M. Cover and A. A. El Gamal. “Capacity theorems for the relay channel,” *IEEE Trans. on Inf. Theory*, vol. 25, p. 572-584, Sept. 1979.
- [13] A. Sendonaris, E. Erkip, and B. Aazhang, “User Cooperation Diversity – Part I: System Description,” *IEEE Trans. on Commun.*, vol. 51, p. 1927-1938, Nov. 2003.
- [14] A. Sendonaris, E. Erkip, and B. Aazhang, “User Cooperation Diversity – Part II: Implementation, Aspects and Performance Analysis,” *IEEE Trans. on Commun.*, vol. 51, p. 1939-1948, Nov. 2003.

- [15] J. N. Laneman, D. N. C. Tse, and G. W. Wornell, "Cooperative Diversity in Wireless Networks: Efficient Protocols and Outage Behavior," *IEEE Trans. on Inf. Theory*, vol.50, no.12, p. 3062-3080, Dec. 2004.
- [16] J. N. Laneman, G. W. Wornell, and D. N. C. Tse, "An Efficient Protocol for Realizing Cooperative Diversity in Wireless Networks," in *Proc. IEEE International Symposium Inf. Theory (ISIT)*, June 2001.
- [17] J. N. Laneman and G. W. Wornell, "Distributed Space-Time Coded Protocols for Exploiting Cooperative Diversity in Wireless Networks," *IEEE Trans. on Inf. Theory*, vol. 49, no. 10, p. 2415-2525, Oct. 2003.
- [18] R. U. Nabar, H. Boelcskei, and F. W. Kneubhueler, "Fading relay channels: Performance limits and space-time signal design," *IEEE J. Sel. Areas Commun.*, vol. 22, p. 1099-1109, Aug. 2004.
- [19] K. Azarian, H. E. Gamal, and P. Schniter, "On the Achievable Diversity-Multiplexing Tradeoff in Half-duplex Cooperative channels", *IEEE Trans. on Inf. Theory*, vol. 51, no. 12, p. 4152 - 4172, Dec. 2005.
- [20] H. J. Strangeways, "Determination of the capacity of ionospheric HF MIMO systems employing linear or planar arrays or co-located antennas", COST 296 Workshop, Oct. 2006
- [21] M. Sharp, A. Scaglino and S. Galli, "Distributed Randomized Space-Time Coding for HF Transmission," *Military communications Conference. MILCOM 2006*, p. 1-6, Oct. 2006.
- [22] Y. Wu and W. Y. Zou, "Orthogonal Frequency Division Multiplexing: A multi carrier modulation scheme," *IEEE*, vol. 41, no.3, August 1995.
- [23] Z. Liu, Y. Xin and G. B. Giannakis, "Linear Constellation Precoding for OFDM with Maximum Multipath Diversity and Coding Gains," *IEEE Trans. on Communications*, vol. 51, no. 3, p. 416-427, 2003.
- [24] S. G. King, Y.M. Ha and E. K. Joo, "A Comparative Investigation on Channel Estimation Algorithms for OFDM in Mobile Communications," *IEEE Trans. Broadcast.*, vol.49, no. 2, p. 142-149, June 2003.

- [25] L. Soyer, "HF Messenger: European trials and R&D efforts", *IEEE Military Communications Conference (MILCOM)*, Oct. 2001.
- [26] J. Tavares, J. Angeja, L. Carvalho, and A. Navarro, "Increasing HF radio communication capacity to support real-time video", *IEEE International Symposium on Consumer Electronics*, June 2005.
- [27] <http://www.drm.org/>
- [28] <http://www.arrl.org/news/stories/2007/02/22/102/?nc=1>
- [29] A. Dowler and A. Nix, "Performance Evaluation of Channel Estimation Techniques in Multiple Antenna OFDM System", *IEEE Vehic. Tech. Conf.*, vol. 2, Orlando, FL, p. 1214-1218, Oct. 2003.
- [30] H. Mheidat, M. Uysal and N. Al-Dahir, "Equalization Techniques for Distributed Space-Time Block Codes With Amplify –and-Forward Relaying", *IEEE Trans. on Signal Processing*, vol.55, no.5, part 1, p. 1839-1852, May 2007.
- [31] ITU, Recommendation 533-1 "Estimating Sky-Wave Field Strength and Transmission Loss at Frequencies Greater than 2 MHz," *Recommendation and Reports of the CCIR*, vol. VI, p.237, Dubrovnik, 1986.
- [32] S. M. Alamouti, "A simple transmit diversity technique for wireless communications," *IEEE Journal on Selected Areas on Communications*, vol. 16, no. 8, p. 1451-1458, October 1998.
- [33] A. Sendonaris, E. Erkip and B. Aazhang, "User cooperation diversity. Part II. Implementation aspects and performance analysis", *IEEE Transactions on Communications*, vol. 51, no.11, p. 1939-1948, Nov. 2003.
- [34] A. Sendonaris, E. Erkip and B. Aazhang, "User cooperation diversity. Part I. System description", *IEEE Transactions on Communications*, vol. 51, no.11, p. 1927-1938 Nov. 2003.
- [35] M. Janani, A. Hedayat, T. E. Hunter and A. Nosratinia, "Coded Cooperation in Wireless Communications: Space-Time Transmission and Iterative Decoding," *IEEE Transactions on Signal Processing*, vol.52, no.2, p. 362-371, Feb. 2004.

- [36] J. K. Cavers, "An Analysis of Pilot Symbol Assisted Modulation for Rayleigh Fading Channels," *IEEE Trans. on Vehic. Tech.*, vol.40, no.4, p. 686-693, Nov.1991.
- [37] V. Tarokh, N. Seshadri, and A. R. Calderbank, "Space-Time Codes for High Data Rates Wireless Communications: Performance Criterion and Code Construction," *IEEE Trans. on Inf. Theory*, vol.44, p.744-765, March 1998.
- [38] S. Hara and P. Ramjee, Multicarrier Techniques for 4G mobile communications, *Artech House*, USA, 2003.
- [39] J. G. Proakis, Digital Communications, 3rd edition, *McGraw-Hill*, New York, 1995.
- [40] W. Jakes, Microwave Mobile Communications, *John Wiley & Sons Ltd.*, England, 1994.